ECS Journal of Solid State
Science and Technology

Investigation of the Electrical Parameters of the Organic Diode Modified with 4-[(3-Methylphenyl)(phenyl)amino] Benzoic Acid

Investigation of the Electrical Parameters of the Organic Diode Modified with 4-[(3-Methylphenyl)(phenyl)amino] Benzoic Acid

A. Kemal Havare,[a,z] M. Can,[b,z] N. Yagmurcukardes,[c] M. Z. Yigit,[d] H. Aydın,[c] S. Okur,[d] S. Demic,[d] and S. Icli[e]

[a]*Toros University, Electrical-Electronics Engineering, Mersin, Turkey*
[b]*Izmir Kâtip Çelebi University, Department of Engineering Sciences, Izmir, Turkey*
[c]*Izmir Institute of Technology, Material Science and Engineering, Izmir, Turkey*
[d]*Izmir Kâtip Çelebi University, Department of Material Science and Engineering, Izmir, Turkey*
[e]*Ege University, Institute of Solar Energy, Izmir, Turkey*

4-[(3-Methylphenyl)(phenyl)amino]benzoic acid (MPPBA) self-assembled monolayer (SAM) molecules as hole injection is formed on p and n type Si and on indium-tin oxide (ITO) electrodes to investigate the effect on the electrical parameters of hole only organic device. The hole mobility improvement of organic device was attributed to an intermediate energy level formed between hole transport materials (HTL) (N,N′-Bis(naphthalen-1-yl)-N,N′-bis(phenyl)benzidine -NPB) and ITO when forming an ultrathin MPPBA layer, leading to increase of carrier mobility of the device. Space charge limited current (SCLC) technique is used to estimate the mobility of the NPB formed at the interface metal/organic Ohmic contact. The hole mobility of ITO/NPB/Al and ITO/MPPBA/NPB/Al devices were obtained as 1.80×10^{-6} and 1.76×10^{-3} cm^2/Vs, at 1350 E $(V/cm)^{1/2}$ applied electric field, respectively. SAM modified devices has lower barrier height values. The electronic characteristic parameters of the ITO/(with or without MPPBA)/NPB/Al, Au/n-Si(or p-Si)/(with or without MPPBA)/Au contacts were calculated using current–voltage (I–V) measurements by Schottky type carrier injection.

 [DOI: 10.1149/2.0131605jss]

Manuscript submitted December 17, 2015; revised manuscript received February 2, 2016. Published February 25, 2016.

In the last three decades, studies focused on improving the performance of organic semiconductors materials for all organic circuits due to low cost, large area applications and flexible displays.[1–4] Recently, organic semiconductors with high charge mobilities have been developed.[5–7] Furthermore, improving the charge injection, enhancing hole mobility to balance the electron-hole at the anode/organic interface play an important role in organic electronic.[2] SCLC, one of the basic method to measure mobility of organic semiconductors (O-SC) contacts, have been carried out to evaluate the carrier mobility between metal contact and O-SC layer.[8–10] In literature, theory of the SCLC and the charges mobilities of O-SC have been studied to measure electrical parameters of the devices.[11,12] When the applied electric field is less than 10^4 V/cm, the amount of charge carriers injected into the organic layer is less than the intrinsic charge carriers fill in the organic layer. If the applied external electric field higher than10^5 V/cm, due to low carrier mobility, near the anode/organic interface the injected current density is higher than the intrinsic charge density therefore the internal electrical carrier is enhanced by the space charges.[13]

Experimental

The Si wafers were imported from Si-Mat with [100] orientation and 5–10 Ωcm resistivity and the ITO was purchased from Sigma Aldrich, with a surface resistivity of 15–25 Ωcm for using as a substrate. As the HTL materials, commercial NPB with 99% sublimed grade from Aldrich were used (Fig. 1) MPPBA were synthesized in order to modify the ITO and Si surface and to facilitate the hole injection.[14]

The chemicals; acetone (CH_3COCH_3 - 99.8%, purchased from Merck), ethanol (C_2H_6O –99.8%, purchased from Sigma Aldrich), and 2-propanol (CH_3CH (OH) CH_3 – 99.8%, purchased from Merck) were used in standard cleaning process for the ITO and Si substrate. The self-assembled monolayer process is formed by simply some steps. The first one is to prepare the solution and the second one is to immerse a substrate into a solution of the surface-active material.

Finally the spontaneous organization of the assembly comprises chemical bond of molecules with the surface and intermolecular interactions. The bare ITO and Si substrate before SAM treatment was cleaned by plasma cleaning. Plasma cleaning system consist of 14% O_2 and 86% Ar gas mixture. The cleaned ITO and Si substrates were kept in the 1 mM ethanol solution of MPPBA at room temperature for 48 hours. A chemical bounding may constitute on the hydroxyl-rich ITO and Si surface due to the active carboxylic acid head group of MPPBA molecules (Fig. 3). The substrates were then rinsed with ethanol to remove the residual MPPBA molecules from the ITO and Si surface and finally SAM modified substrates were dried in a stream of N_2 gas. The Si substrates are separately cleaned by a deionized water (DI) rinse, followed by a dilute 2% HF dip then DI rinse and blow dry. After that the gold (Au) material as an ohmic contact was evaporated onto Si substrates under 10^{-6} Torr to obtain the Au/n-Si or p-Si/MPPBA structure separately. As a final step to constitute the Au/n-Si(or p-Si)/(with or without MPPBA)/Au structure, the gold was evaporated. On the other hand the SAM modified ITO substrates were placed in organic evaporation system and the NPB organic HTL materials were deposited under 10^{-6} Torr vacuum. The NPB layer was evaporated with 0.5 Å/s deposition rate as 50 nm. Finally, Al was evaporated as contact electrode (120 nm) at a pressure of 4×10^{-6} Torr and a deposition rate of 3 Å/s in thermal evaporation system to obtain the device (Fig. 2a). The several devices with and without the SAM is ready to obtain electrical data of each type.

The surface morphology of the thin films was characterized by Solver Pro AFM from NTMDT. The topography and the phase contrast images of the samples were taken using NSG10 type of silicon tip with 30 ± 5 μm cantilever width and typical 240 kHz resonant frequency. Chemical structures of the used MPPBA-SAM molecule and NPB-HTL materials are shown in Fig. 1.

Results and Discussion

In organic electronics device, charge transport and the charge injection is obtained with the inter-site hopping from delocalized states in electrode to localized states in the organic layer.[15] The transition rate is related with the energy difference and distance between the layers. The lowest unoccupied molecular orbital (LUMO) and highest occupied molecular orbital (HOMO) are occurred by the energy states that are involved in the transport of holes and electrons. SCLC type

[z]E-mail: alikemal.havare@toros.edu.tr; mustafacan80@yahoo.com

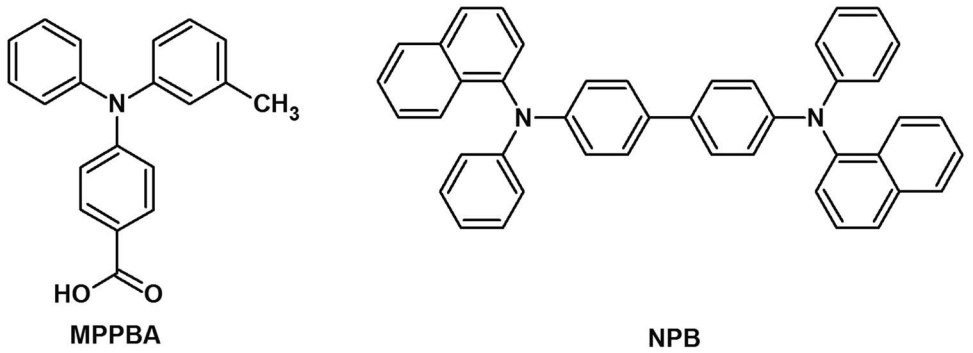

Figure 1. Chemical structures of used MPPBA and NPB materials, respectively.

mechanism explain the conduction in device where strong injection is achieved from both electrodes[16,17]

When an external electric field is applied to the electrodes, holes are injected from anode ITO into the HTL and drift across it. As the hole mobility is lower in the electron transport layer (ETL), motion of the holes slows down at the interface. According to Haichaun Mu, the same mechanism is also valid for electrons as they cross organic/organic interface, which leads to substantial charge accumulation at the interface.[18] Base on previous study,[14] an interface dipole exist between ITO and organic layer (Fig. 3). As well as there is potential energy barrier between ITO and HOMO level of HTL-NPB round about 0, 7 eV (Fig. 2b). Formed the MPPBA layer on ITO constitute an energy level as a step lower than HOMO level of HTL. Thus it decreases energy barrier between HOMO level of HTL and anode electrode about 0.29 eV. So that the MPPBA layer assistance the hole injection from ITO to HOMO level of HTL easily.

The identical approach for the Au/n-Si(or p-Si)/MPPBA/Au device, the MPPBA (SAM) layer(s) chemically also bond to the surface of the Silicon (native oxide) substrate by carboxylic acids allowing for direct charge transport and charge injection though the molecules.[19–21] The presence of a voltage increases the current due to the charges transport takes place via through-π conjugated bond tunneling assisted by the bond π-π* transition.[22–24] Further increases in voltage means increases the electric field leads to the charges tunneling through the SAM molecule. In addition the surface potential energy of the Si substrate changes by modifying via SAM layer leads to the work function of Au/n-Si/MPPBA changes and comes to 5.09 eV (Fig. 3). The presence of MBBA layer which reduce the work function differences between n-Si and Au[25] enhance the current of the SAM modified device more than unmodified device. The hole injection through MPPBA is increased by constituted energy levels between n-Si and Au energy bands (Fig. 3). The potential energy differences reduce to from 1.05 eV to 0.11 eV. Therefore, the I-V behavior of Au/n-Si/MPPBA/Au device shows higher current than bare one, n-Si/Au (Fig. 7). From the view of this point the higher current enables to have lower series resistance. That is why the series resistance (Rs) of n-Si/Au devices higher than that of n-Si/MPPBA/Au devices.

Surfaces characterization by atomic force microscopy.—The surface of the bare ITO and SAM modified ITO is investigated by AFM technique in high-resolution (Fig. 3). The surface roughness or root mean square (rms) of the bare ITO was measured as 3.71 nm. From the height images it is clear that bare ITO exhibit rough and grain like surface morphology.

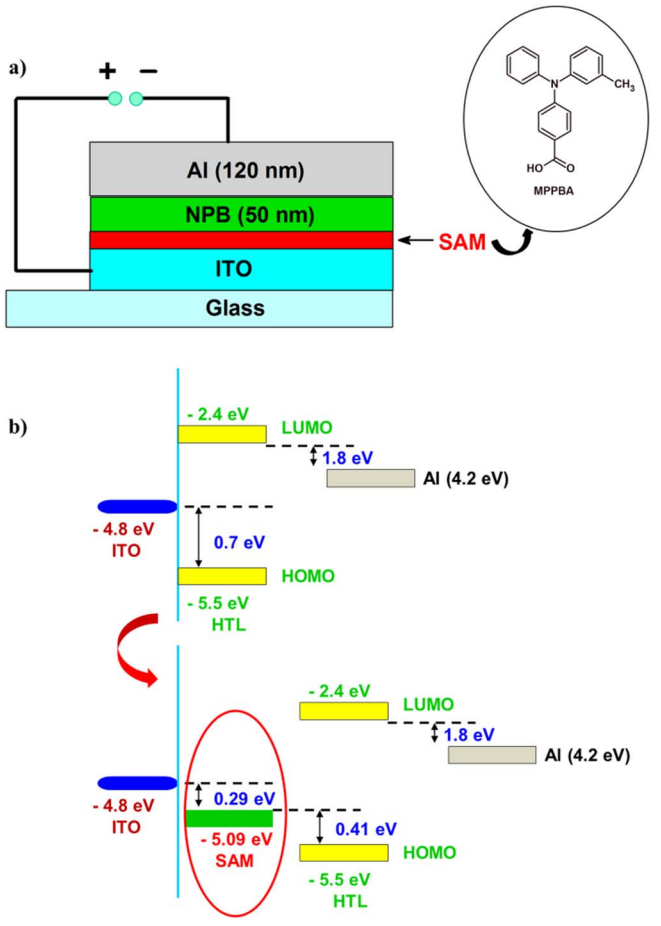

Figure 2. Device structure ITO/MPPBA/NPB/Al[14] (a) and energy level diagram of ITO, MPPBA-SAM and NPB-HTL (b).

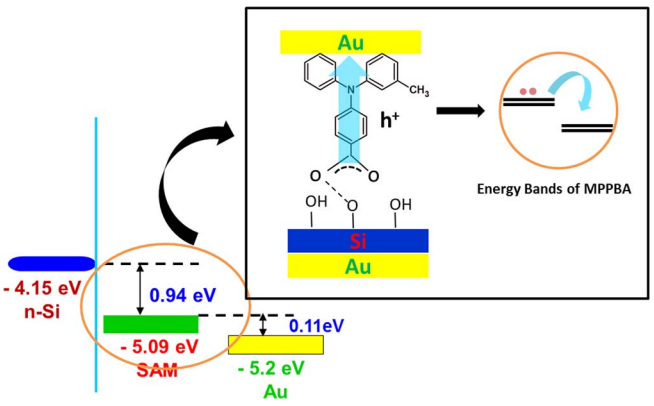

Figure 3. The Energy band diagram of Au/n-Si/MPPBA/Au structure and the hole injection through π conjugated MPPBA molecule.

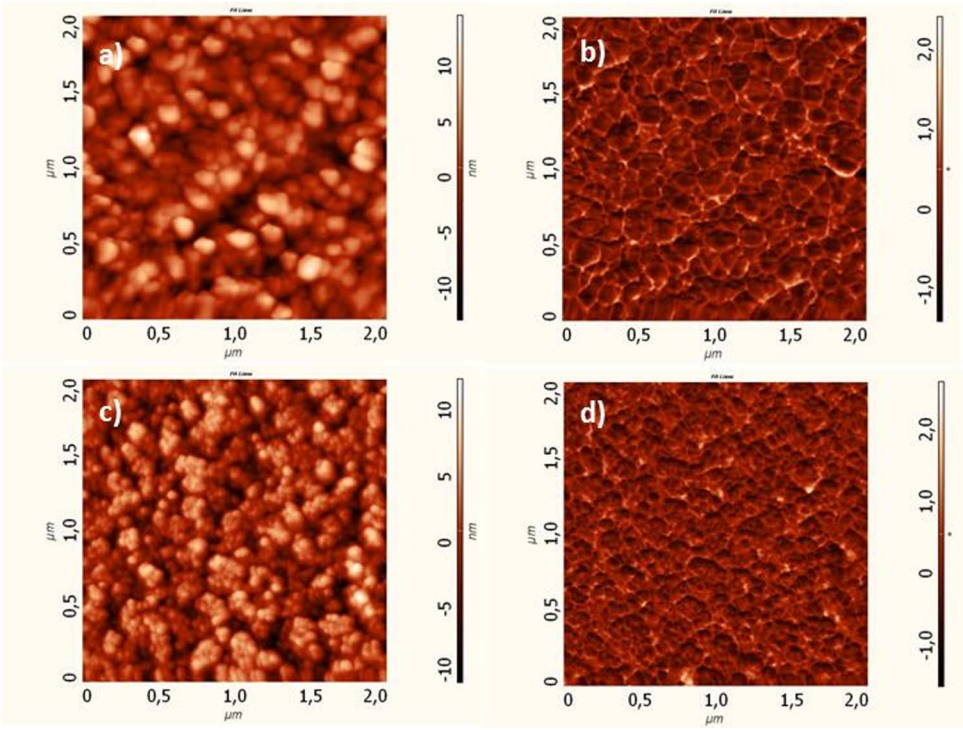

Figure 4. (a) The surface topography and (b) phase contrast images of the bare ITO surface. (c) the surface topography and (d) phase contrast images of the MPPBA modified ITO.

The rms value of the SAM modified ITO surface is 3.41 nm. As a result, SAM modified ITO surface shows lower roughness compare to bare ITO surface, which is beneficial for the hole's injection. Moreover, the phase images indicate some island structures are formed on the surface by the SAM modification with respect to the bare ITO (Fig. 4b). It is especially convenient in analyzing polymers such as SAMs, composites and surface coatings. The surface image of NPB coated on bare or MPPBA modified ITO surface are shown in Fig. 4. The MPPBA forms as organic buffer layer on ITO surface structure. In addition, MPPBA molecules have similar molecular structure to overlaying NPB (Fig. 1). This give rise to well matching with NPB structure at the interface. That's because, NPB coated films have lower surface roughness compare to unmodified NPB films. From the phase image (Figs. 5b and 5d), MPPBA molecule exhibited a well dispersed NPB films with respect to the bare ITO.

NPB coated substrates have smoother surfaces with roughness of 2.22 nm. The final ITO/MPPBA/NPB device rms values decreased to 1.92 nm significantly. Thus, MPPBA layer lead to have a smoother surface by filling the concaves of ITO surface. As a result, lower RMS roughness is the key reasons for improved mobility in the devices.[26] The roughness values of fabricated thin films summarize in the Table I.

Electrical parameters of the devices.—In this study, we used novel MPPBA self-assembled aromatic molecules on ITO or on n-Si (p-Si) surface to compare the effect of SAM layers on the electronic parameters of organic diodes, fabricated ITO/(with or without MPPBA)/NPB/Al, Au/n-Si(or p-Si)/(with or without MPPBA)/Au devices. The electrical characteristics of the devices were measured with Keithley 2400 source meter in air at room temperature. Electrical parameters of the devices were investigated using forward-bias current-voltage (I-V) measurements (Fig. 6 and Fig. 7). As the voltage is applied between two electrodes, holes are injected into the ITO and transport HOMO level of NPB whereas electrons are injected into Al cathode and transported LUMO level of Hole Transport Layer (HTL). MPPBA (SAM) and NPB materials is known as a HTL and hole injection material. By modification of anode ITO surface via MPPBA the potential barrier changes and the work function of ITO is reduced. So that the barrier between HOMO level of NPB and anode ITO (0.29 eV) becomes very small comparing with the differences LUMO level of NPB and cathode (1.8 eV) (Fig. 2). That is because the holes inject easier and the device behaves as hole-only. However those of the ITO/MPPBA/NPB/Al and ITO/NPB/Al structures show slight 'soft' behavior in which the current does not saturate to a constant value (Fig. 6). On the other hand the I-V curves of ITO/MPPBA/NPB/Al and ITO/NPB/Al exhibits that the forward bias threshold is higher than reverse bias current comparing with the ITO/MPPBA/Al. As a result, this rectifying behavior is the basis of the diode characteristics.

To investigate the variations caused by MPPBA molecules in different structures, MPPBA modified n and p-type silicon substrates were used. In Fig. 7 the current-voltage relation of bare n-type silicon and MPPBA modified n-type silicon is shown. Under forward bias, the current of the MPPBA modified silicon device is higher than the bare silicon. This observation indicates that the use of SAM molecules can improve charge injections.

The I-V characteristics of Au/n-Si/Au structure is exhibited as a diode behavior and restricted by the magnitude of the potential barrier at the hetero-interface and the properties of the Si substrate. When external electric field is applied to the electrodes, electrons are injected into the n- type Si, holes are injected into the SAM molecule and forms typically diode I-V characteristic as indicated in Fig 7. The diode behavior is like a Schottky or a metal–semiconductor contact at the low current. The current regime of the diode is thermionic emission at low current.[27,28] At high current, space-charge injection across the MPPBA layer is dominant and is limited by charged states at the contact metal/MPPBA interface, that is, in the case, the current is called the space charged limited current (SCLC). The energy band structure of the n-Si (or -Si)/MPPBA/Au device is given in Fig. 8. The potential barrier in the semiconductor is reduced by SAM layer (Fig. 8), the charges are "driven" across the barrier so that a large net current from the semiconductor into the metal results. The forward I-V characteristics of the device also show the rectifying behavior (Fig. 7) and the reverse curves of the Au/n-Si (or p-Si)/MPPBA/Au structure

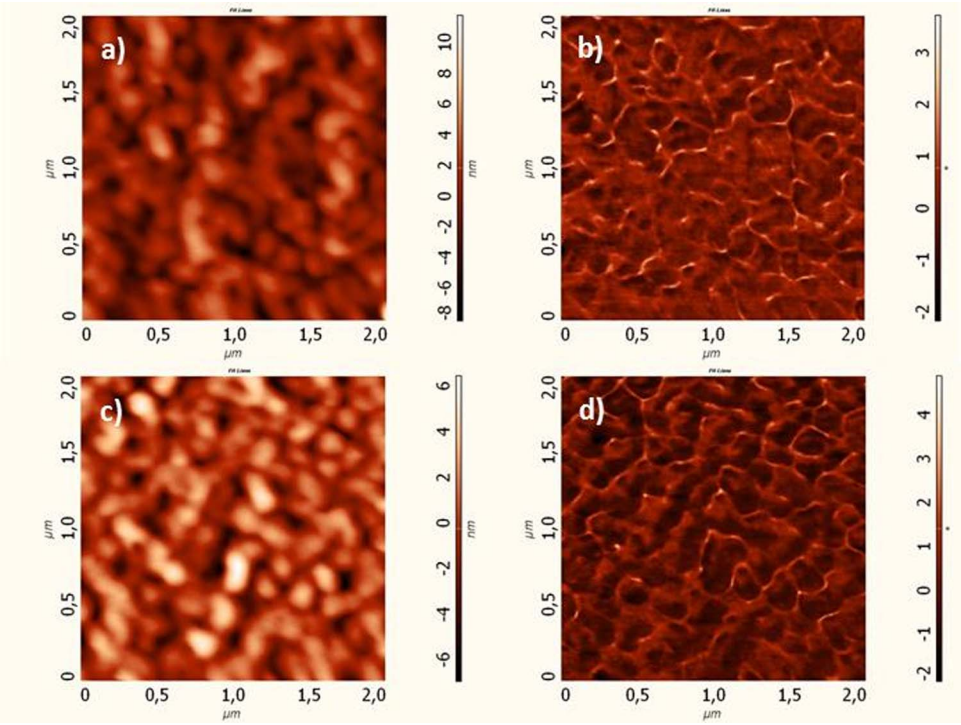

Figure 5. (a) The surface topography and (b) phase contrast images of the bare ITO surface coated NPB (c) the surface topography and (d) phase contrast images of the MPPBA modified ITO surface coated NPB.

Table I. The surface roughness values of the thin films.

Thin Films	Roughness (rms)(nm)
Bare ITO	3.71
ITO/MPPBA	3.41
ITO/NPB	2.22
ITO/MPPBA/NPB	1.92

exhibits the excellent saturation, but the ITO/MPPBA/NPB/Al and ITO/NPB/Al structures show slight 'soft' behavior in which the current does not saturate to a constant value (Fig. 6).

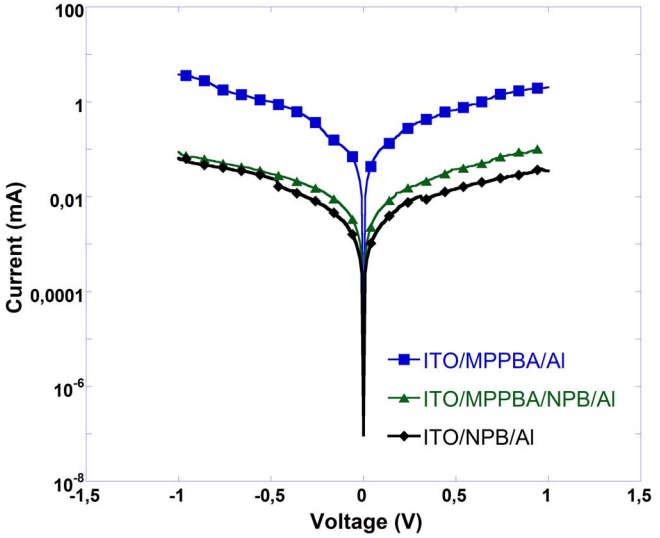

Figure 6. Current-Voltage behavior of ITO/MPPBA/Al, ITO/MPPBA/NPB/Al and ITO/NPB/Al devices.

Schottky type carrier injection is based to characterize the electrical parameters of the devices such as ideality factor (n) and barrier height $\emptyset_B$. The electrons from the electrode can be injected as Schottky injection when suitable thermal energy needed to cross the barrier height is acquired. The current-voltage characteristics for $q(V\text{-}Rs) > kT$ values of the diodes can be analyzed by the relation;[29,30]

$$I = I_0 exp\left(\frac{q\,(V - I R_s)}{nkT}\right) \quad [1]$$

where q the electron charge, k is the Boltzmann's constant, T is the temperature, and V is the applied voltage, R_s is the series resistance, I_0 is saturation current and expressed as:

$$I_0 = AA^*T^2 exp\left(-\frac{q\emptyset_B}{kT}\right) \quad [2]$$

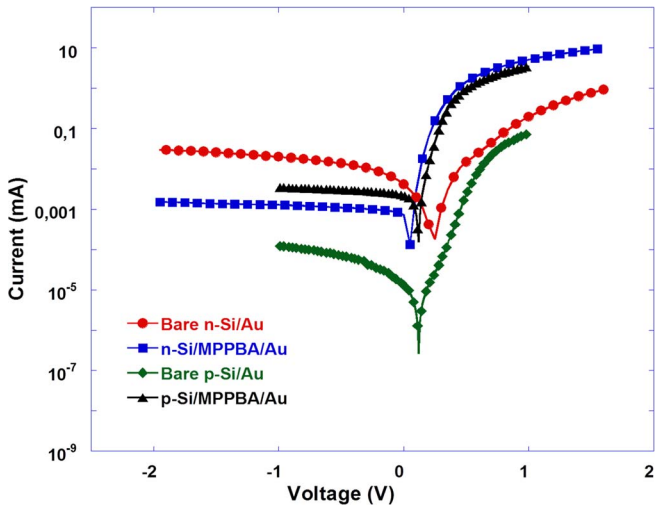

Figure 7. Current-Voltage behavior of bare n-type and p-type silicon, MPPBA modified n-type and p-type silicon.

Table II. Calculated the barrier height and the ideality factors values of devices with NPB organic layer.

Thin Films	Ideality factor (n)	Barrier height (ΦB) (eV)
bare n-Si/Au	1.00	0.67
n-Si/MPPBA/Au	2.70	0.36
bare p-Si/Au	3.38	0.53
p-Si/MPPBA/Au	2.48	0.59
ITO/MPPBA/Al	2.02	0.51
ITO/NPB/Al	2.20	0.61
ITO/MPPBA/NPB/Al	3.61	0.27

Φ_B is the barrier height, A^* is the effective Richardson constant; A is the effective contact area, if rearrange Eq. 2 it gives

$$V = n\frac{kT}{q}\ln\left(I_0\frac{AA^*}{T^2}\right) + n\phi_B + IR_s \quad [3]$$

If Eq. 3 differentiated with respect to I, obtained

$$\frac{dV}{d\ ln\ (I)} = n\frac{kT}{q} + IR_s \quad [4]$$

The saturation current obtained from the linear portion intercept of *log I* at zero voltage. The ideality factor and barrier height values of the four diodes were calculated from the slope of the linear region and y-axis intercept of the forward bias *ln(I)-V* curve. The obtained ideality factors that higher than unity indicates that diodes show non-ideal behavior because of the interface layer and series resistance. This significant series resistance effect can be analyzed by Cheung's functions.[31] The current-voltage behavior of bare p- and n-type silicon is shown in Fig. 6. MPPBA modified p-type silicon device has a better rectification behavior than bare p-type device in the both reverse bias and forward bias region. The barrier height values and the ideality factor of untreated n- and p-type devices and MPPBA modified n- and p-type devices are shown in Table II. It is obvious from the barrier height values, that SAM modification of the silicon substrates alters the surface properties of the devices.

I-V characteristics of fabricated ITO/MPPBA/Al, ITO/MPPBA/NPB/Al and ITO/NPB/Al devices are shown in Fig. 6. The plots are obtained symmetric at negative and positive applied voltage intervals. The ideality factor and barrier height by Cheung relation is presented in Table II. The barrier height values of the fabricated devices are close to each other but the ideality factor results vary at different devices. SAM modification reduces the difference between the bare ITO and NPB coated ITO in current-voltage plots.

Hole mobility by SCLC.—The electrical characteristics indicate two distinct regions at low and high biases relatively. As the voltage increases the electrical characteristics turn to space charge limited current (SCLC) and SCLC can be expressed as[32]

$$J_{SCLC} = \frac{9}{8}\varepsilon\varepsilon_0\mu\frac{V^2}{L^3} \quad [5]$$

where ε the relative dielectric constant, V voltage, ε_0 the dielectric constant, L the sample thickness and μ is the field independent charge carrier mobility. The carrier mobility is influenced by energetic disorder owing to the interaction of each hopping charge with randomly oriented and located dipoles in the organic thin film.[33] The mobility is dependent on the electric field can be formulated by a Poole-Frenkel equation,

$$\mu(E) = \mu_0\exp(\beta\sqrt{E}) \quad [6]$$

where μ_0 is the zero field mobility and β is the Poole-Frenkel factor. So that from Eq. 5 and Eq. 6, the field dependent SCLC can be given by

$$J_{SCLC} = \frac{9}{8}\varepsilon\varepsilon_0\frac{V^2}{L^3}\mu_0\exp(\beta\sqrt{E}) \quad [7]$$

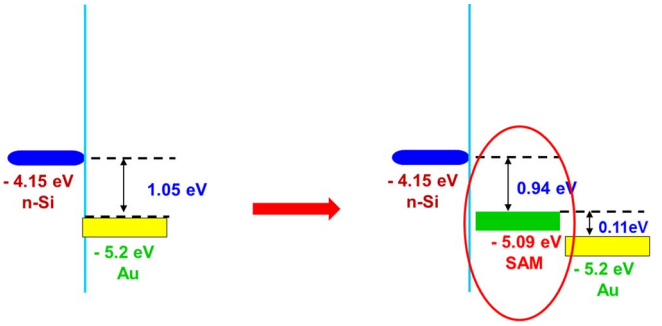

Figure 8. Energy level diagram of n-Si /MPPBA/Au device.

To evaluate the carrier mobility under steady state current in an organic semiconductor, space-charge-limited current (SCLC) measurements were done for the current-voltage behavior of ITO/NPB/Al and ITO/MPPBA/NPB/Al devices.

The comparison of the logarithmic graphs of J/E^2 versus the square root of the applied electric field $[E\ (V/cm)]^{1/2}$ for ITO/NPB/Al and ITO/MPPBA/NPB/Al devices are shown in Fig. 9a and it is compatible with literature.[34] The slope and the intercept give β, the Poole-Frenkel factor and zero-field mobility μ_0, the relative dielectric constant ε of organic material is assumed to be 3,[35–39] and the permittivity of the free space ε_0 is 8.85×10^{-12}.[34] As well as the calculated carrier mobility versus the square root of the applied electric field plots $[E\ (V/cm)]^{1/2}$

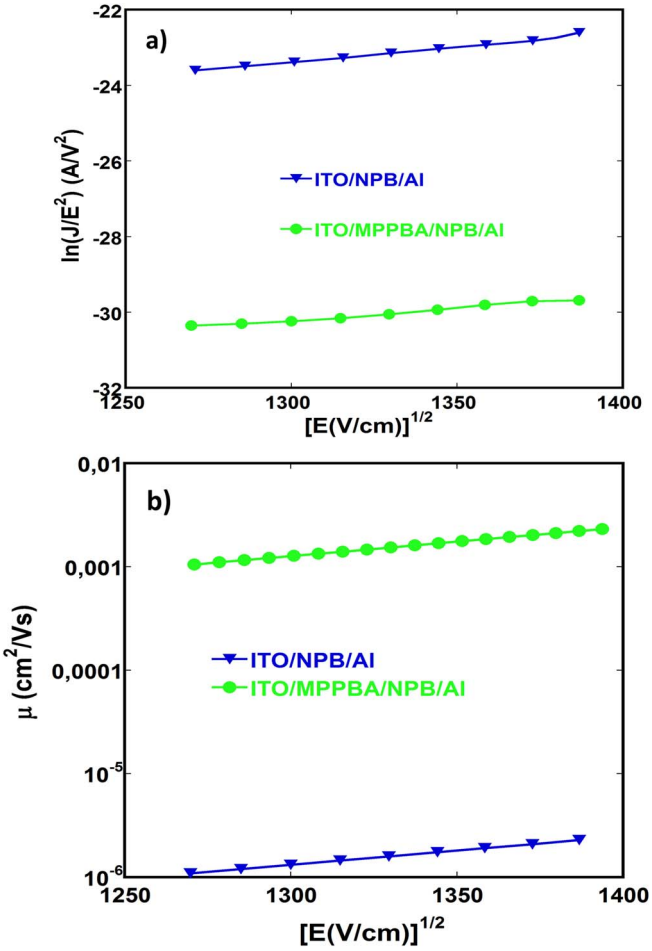

Figure 9. The logarithm of J/E^2 versus the square root of the applied electric field for ITO/NPB/Al and ITO/MPPBA/NPB/Al devices (a), the carrier mobility of ITO/TPD/Al and ITO/MPPBA/TPD/Al devices (b).

Table III. Calculated hole mobility values of the fabricated devices.

Devices	μ (cm^2/V_s)
ITO/NPB/Al	1.803×10^{-6}
ITO/MPPBA/NPB/Al	1.769×10^{-3}

of ITO/NPB/Al and ITO/MPPBA/NPB/Al devices are shown in Fig. 9b. The hole mobility of ITO/NPB/AL and ITO/MPPBA/NPB/Al devices were calculated as 1.803×10^{-6} and 1.769×10^{-3} cm^2/Vs at 1350 E $(V/cm)^{1/2}$ applied electric field, respectively. The space charge limited current analysis shows that the injected current is proportional to charge mobility which is of NPB hole transport material on ITO increases with the use of carboxylic MPPBA self-assembled monolayer.[40]

Calculated charge carrier mobility values of fabricated devices at are summarized in the Table III.

Summary

The SAM modified hole only device showed a significant enhancement performance of comparing to the corresponding bare ITO in terms of electrical parameters and surface characterization. Surface morphology of bare ITO has rougher surface with surface roughness of 3.71 nm. With the MPPBA SAM modification, the roughness of the ITO surface decreases to 3.41 nm. NPB coated substrates rms values decreased and have smoother surfaces with surface roughness of 1.92 nm and 2.22 nm for ITO/MPPBA/NPB and ITO/NPB, respectively. Space-charge-limited current (SCLC) analysis showed that carrier mobility is improved under steady state of current in an organic layer by interlayer MPPBA. It is frankly to understand from hole mobility values and indicate that with the SAM modification, charge injection from anode to the organic layer improved under applied electric field.

Acknowledgments

This work was supported by TUBITAK under grant No TBAG-108T718.

References

1. M. Baldo, D. O'brien, Y. You, A. Shoustikov, S. Sibley, M. Thompson, and S. Forrest, *Nature*, **395**, 151 (1998).
2. Z. Chen, J. Yu, Y. Sakuratani, M. Li, M. Sone, S. Miyata, T. Watanabe, X. Wang, and H. Sato, *Journal of applied physics*, **89**, 7895 (2001).
3. V.-E. Choong, S. Shi, J. Curless, C.-L. Shieh, H.-C. Lee, F. So, J. Shen, and J. Yang, *Applied Physics Letters*, **75**, 172 (1999).
4. C.-A. Di, G. Yu, Y. Liu, X. Xu, Y. Song, and D. Zhu, *Applied Physics Letters*, **90** (2007).
5. D. Braga, M. Campione, A. Borghesi, and G. Horowitz, *Advanced Materials*, **22**, 424 (2010).
6. Z. An, J. Yu, S. C. Jones, S. Barlow, S. Yoo, B. Domercq, P. Prins, L. D. Siebbeles, B. Kippelen, and S. Marder, *Advanced Materials*, **17**, 2580 (2005).
7. M. Orrit and J. Bernard, *Phys Rev Lett*, **65**, 2716 (1990).
8. P. W. M. Blom, M. J. M. de Jong, and J. J. M. Vleggaar, *Applied Physics Letters*, **68**, 3308 (1996).
9. L. Bozano, S. Carter, J. Scott, G. Malliaras, and P. Brock, *Applied Physics Letters*, **74**, 1132 (1999).
10. Z. Lü, Z. Deng, J. Zheng, Y. Zou, Z. Chen, D. Xu, and Y. Wang, *Physica E: Low-dimensional Systems and Nanostructures*, **41**, 1806 (2009).
11. T. Matsushima and H. Murata, *Applied Physics Letters*, **95**, 203306 (2009).
12. T. Yasuda, Y. Yamaguchi, D. Zou, and T. Tsutsui, *Japanese journal of applied physics*, **41**, 5626 (2002).
13. A. Singh, Thapar University.
14. A. K. Havare, M. Can, S. Demic, S. Okur, M. Kus, H. Aydin, N. Yagmurcukardes, and S. Tari, *Synthetic Metals*, **161**, 2397 (2011).
15. C. Karnutsch, *Low Threshold Organic Thin Film Laser Devices*, Cuvillier Verlag (2007).
16. T. Yasuda, Y. Yamaguchi, D.-C. Zou, and T. Tsutsui, *Japanese journal of applied physics*, **41**, 5626 (2002).
17. M. Abkowtz and D. Pai, *Philosophical Magazine B*, **53**, 193 (1986).
18. H. Mu, University of Cincinnati (2007).
19. M. A. Reed, C. Zhou, M. Deshpande, C. Muller, T. Burgin, L. Jones, and J. M. Tour, *Annals of the New York Academy of Sciences*, **852**, 133 (1998).
20. V. Burtman, A. Zelichonok, and A. V. Pakoulev, *International journal of molecular sciences*, **12**, 173 (2011).
21. S. A. DiBenedetto, A. Facchetti, M. A. Ratner, and T. J. Marks, *Adv Mater*, **21**, 1407 (2009).
22. K. Ishizuka, M. Suzuki, S. Fujii, Y. Takayama, F. Sato, and M. Fujihira, *Japanese journal of applied physics*, **45**, 2037 (2006).
23. W. Wang, T. Lee, and M. A. Reed, *Physical Review B*, **68**, 035416 (2003).
24. L.-L. Chua, J. Zaumseil, J.-F. Chang, E. C.-W. Ou, P. K.-H. Ho, H. Sirringhaus, and R. H. Friend, *Nature*, **434**, 194 (2005).
25. Y. Ge, *Chemical and electronic properties of semiconducting oligomer and thiol monolayer interfaces*, ProQuest (2008).
26. F. Li, A. Nathan, Y. Wu, and B. S. Ong, *Organic thin film transistor integration: A hybrid approach*, John Wiley & Sons (2011).
27. M. Cakar, C. Temirci, and A. Türüt, *Synthetic Metals*, **142**, 177 (2004).
28. F. Yakuphanoglu, M. Kandaz, and B. Senkal, *Thin Solid Films*, **516**, 8793 (2008).
29. S. Sze, Wiley, New York (1981).
30. E. H. Rhoderick and R. Williams, *Metal-semiconductor contacts*, Clarendon Press, Oxford (1988).
31. S. Cheung and N. Cheung, *Applied Physics Letters*, **49**, 85 (1986).
32. M. Khan, W. Xu, Y. Bai, X. Jiang, Z. Zhang, and W. Zhu, *Journal of applied physics*, **103**, 014509-014504 (2008).
33. J. Xueyin, Z. Zhilin, Z. Xiaowen, Z. Liang, and L. Jun, *Journal of Semiconductors*, **30**, 114009 (2009).
34. P. Stallinga, *Front Matter*, Wiley Online Library (2009).
35. M. Khan, W. Xu, Y. Bai, F. Wei, X. Jiang, Z. Zhang, and W. Zhu, *Journal of Physics D: Applied Physics*, **40**, 6535 (2007).
36. P. Kumar, S. Jain, V. Kumar, A. Misra, S. Chand, and M. Kamalasanan, *Synthetic Metals*, **157**, 905 (2007).
37. M. Khan, W. Xu, X. W. Zhang, Y. Bai, X. Jiang, Z. Zhang, and W. Zhu, *Journal of Physics D: Applied Physics*, **41**, 225105 (2008).
38. W. Brütting, S. Berleb, and A. G. Mückl, *Organic electronics*, **2**, 1 (2001).
39. A. Campbell, M. Weaver, D. Lidzey, and D. Bradley, *Journal of applied physics*, **84**, 6737 (1998).
40. Y. Shen, M. W. Klein, D. B. Jacobs, J. C. Scott, and G. G. Malliaras, *Physical review letters*, **86**, 3867 (2001).